Laser spectroscopy of Pr^{3+} ions in $LiKY_{1-x}Pr_xF_5$ single crystals

R. Balda, J. Fernández, I. Saéz de Ocáriz, M. Voda, and A. J. García
Departamento de Física Aplicada I, E.T.S.I.I. y Telecom., Universidad del País Vasco, Alameda Urquijo s/n, 48013, Bilbao, Spain

N. Khaidukov
Kurnakov Institute of General and Inorganic Chemistry, Russian Academy of Sciences, Moscow, Russia
(Received 23 June 1998; revised manuscript received 17 August 1998)

The visible luminescence of Pr^{3+}-doped fluoride $LiKY_{1-x}Pr_xF_5$ crystals ($x=0.001$, 0.01, 0.02, 0.03, 0.05, and 0.1) has been investigated as a function of concentration and temperature by using time-resolved laser spectroscopy. The temperature-dependent concentration quenching of the $^3P_0$ fluorescence in the 10–77 K temperature range can be described in the framework of a thermally activated cross-relaxation process involving the $^1D_2$ and $^3H_6$ states. However, the single exponential character of the decays at all concentrations and temperatures suggests that energy migration is also present in this system. The fluorescence from the $^1D_2$ level shows a strong concentration quenching for Pr^{3+} concentrations higher than $x=0.001$ even at 4.2 K. The time evolution of the decays from the $^1D_2$ state for concentrations higher than $x=0.001$ is consistent with a dipole-dipole energy transfer mechanism. Anti-Stokes emission from the $^3P_0$ level following excitation of the $^1D_2$ state is also studied for different Pr^{3+} concentrations. Analysis of the upconverted fluorescence decays supports that the mechanism responsible for the upconvertion process is energy transfer. However, this process seems to be complex enough to allow for the use of a single model which could explain the behavior observed. [S0163-1829(99)04615-9]

I. INTRODUCTION

The luminescence of rare-earth ions has been intensively investigated in different host materials, due to the important applications in lasers and nonlinear optics. Among rare-earth ions, trivalent praseodymium is an attractive optical activator, because its energy level spectrum contains several metastable multiplets $^3P_{0,1,2}$, $^1D_2$, $^1G_4$ that offer the possibility of simultaneous emission in the blue, green, orange, red, and infrared wavelengths.[1] The spectroscopic behavior and laser properties of Pr^{3+} were investigated in different types of crystalline hosts. Laser action has been reported for Pr^{3+} ions in different crystals such as $YAlO_3$, YAG, $LaCl_3$ as well as in optical fibers.[2–5] Furthermore, up-conversion lasing under infrared excitation has been demonstrated in Pr^{3+}-doped systems,[6,7] which is very interesting for the development of compact systems using infrared laser diode pumping devices.

Anisotropic fluoride crystals are also promising host materials for rare-earth ions because of their optical properties such as good transparency from the ultraviolet to the infrared region of the spectrum, low optical nonlinearities, and low phonon energies. In recent years stimulated emission of Pr^{3+} ions was also observed in the anisotropic $LiYF_4$, PrF_3, BaY_2F_8, and $LiLuF_4$ crystals.[8–11] Recently, Kaminskii *et al.*[12] reported the spectroscopy and laser action of anisotropic single centered $LiKYF_5$:Nd^{3+} crystals grown by the hydrothermal method. More recently, Nicholls *et al.*[13] reported the laser and spectroscopic properties of Nd^{3+} doped $LiKYF_5$ and $LiKGdF_5$ crystals grown by the top seeded solution growth.

The $LiKYF_5$ compound crystallizes in the monoclinic system (space group $P2_1/c$) with lattice parameters $a=0.62925$ nm, $b=1.1747$ nm, $c=0.64699$ nm, and $\beta \approx 113.7°$ (Ref. 12). The Y^{3+} site is eightfold coordinated to F^- ions and has C_2 point symmetry. These crystals are transparent in the spectral region from 0.15 to 8.5 μm. According to the Raman-scattering measurements the maximum energy of optical phonons for these crystals is equal to ≈ 440 cm^{-1}. Spectroscopic and lasing investigations of these crystals doped with Nd^{3+} ions show that Nd^{3+} substitutes Y^{3+} ions to form one type of activator center in hydrothermal grown crystals.[12]

As far as we know, there does not exist any optical characterization of Pr^{3+} ions in $LiKYF_5$ crystal. This work presents, together with a detailed study of the optical properties of Pr^{3+} ions, a dynamical study of the different energy transfer mechanisms present in $LiKY_{1-x}Pr_xF_5$ crystals. The study includes absorption and emission properties, lifetimes, time resolved emission spectra, fluorescence quenching processes, and frequency up-conversion. The fluorescence dynamics of the $^3P_0$ and $^1D_2$ levels has been analyzed from the luminescence decay curves as a function of concentration and temperature and some conclusions about the mechanisms responsible for the nonradiative relaxations can be inferred. Additional information concerning the ion-ion interaction processes was obtained by means of the study of the anti-Stokes emission from the $^3P_0$ level after excitation of the $^1D_2$ state.

II. EXPERIMENTAL TECHNIQUES

The series of single crystals $LiKY_{1-x}Pr_xF_5$ (with the nominal concentrations $x=0.001$, 0.01, 0.02, 0.03, 0.05, and 0.1) was obtained by a hydrothermal technique.[12,14] The fluorides were synthesized by a direct temperature gradient method as a result of the reaction of aqueous solutions of KF

(20–25 mol %) and LiF whose mole ratio KF/LiF changed from 4.8 to 5.2 with appropriate mixtures of yttrium and praseodymium oxides (99.995% pure) at a temperature of about 750 K, a temperature gradient of about 2 K/cm, and pressures of 100–150 MPa. For the hydrothermal experiments, autoclaves with copper liners having a volume of about 40 cm^3 were utilized. Under these conditions spontaneously nucleated crystals up to 0.5 cm^3 in size were grown in the upper region of the autoclave. The phase homogeneity of the obtained crystals and the perfection of the crystal lattice were tested by the x-ray powder difracction method.[14–16]

The samples temperature was varied between 4.2 and 300 K with a continuous flow cryostat. Conventional absorption spectra were performed with a Cary 5 spectrophotometer.

Time-resolved fluorescence spectra were performed by exciting the samples with a pulsed frequency doubled Nd:YAG pumped tunable dye laser of 9 ns pulse width and 0.08 cm^{-1} linewidth, and detected by an EGG-PAR optical multichannel analyzer. For lifetime measurements, the fluorescence was analyzed with a 1 m Spex monochromator, and the signal was detected by a Hamamatsu R928 photomultiplier. Data were processed by an EGG-PAR boxcar integrator.

Experiments under pulsed excitation on the $^1D_2$ level were performed by using a high-power optical parametric oscillator (MOPO, Spectra Physics model 730) which provides 10 ns pulses of about 35 mJ of average energy with a repetition rate of 10 Hz. The luminescence was dispersed by a 500 M SPEX monochromator (spectral resolution ≈0.05 nm) and detected with a cooler photomultiplier. The signals were recorded by using a SR400 two-channel gated photon counter. The decay time measurements were performed by using the averaging facilities of a Tektronix 2400 digital storage oscilloscope.

III. RESULTS AND DISCUSSION

A. Absorption and emission properties

The room-temperature absorption spectra were obtained for all samples in the 200–2500 nm range by making use of a Cary 5 spectrophotometer. The spectrum consists of several bands corresponding to transitions between the $4f^2$ configuration of Pr^{3+} ions. The positions of the bands and the corresponding bandwidths do not change with increasing concentration, indicating that the dopants are homogeneously distributed. Figure 1 shows the simplified energy level diagram showing the positions of the J states of the Pr^{3+} ions in these crystals derived from the absorption spectra. The position of the $^3H_5$ band inferred from the emission spectra is also included.

In order to estimate the content of praseodymium in the different samples, we have calculated the integrated absorption coefficient for different absorption bands and a linear dependence on concentration was found, which indicates that the relative concentrations of Pr^{3+} are in agreement with the nominal values.

The time-resolved emission spectra of Pr^{3+} in $LiKY_{1-x}Pr_xF_5$ were obtained at 4.2 K for all concentrations in the 470–800 nm spectral range by exciting the samples into the $^3H_4 \rightarrow {}^3P_0$ transition, and collecting the luminescence at different time delays after the laser pulse. After

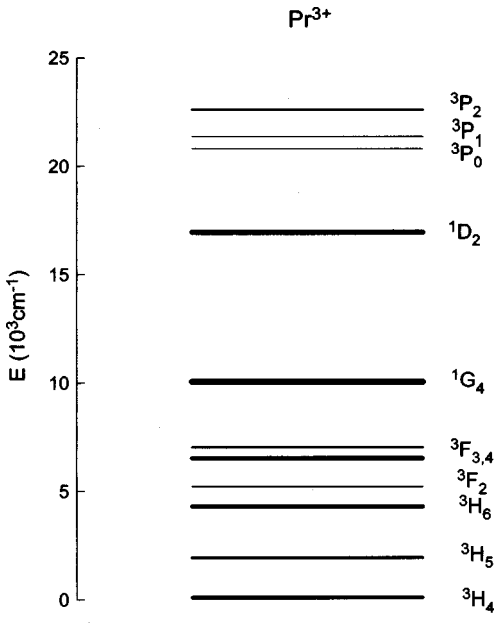

FIG. 1. Energy levels diagram of Pr^{3+} in $LiKY_{1-x}Pr_xF_5$ fluoride crystal (from the absorption data).

excitation in the $^3P_0$ level, luminescence was observed mainly from this level. Figure 2 shows, as an example, the emission spectrum of Pr^{3+} ions for $x=0.001$, corresponding to the $^3P_0 \rightarrow {}^3H_{4,5,6}$ and $^3P_0 \rightarrow {}^3F_{2,3,4}$ transitions obtained at 1 μs after the laser pulse. In addition to the fluorescence from the $^3P_0$ level the emission shows some peaks corresponding to $^1D_2 \rightarrow {}^3H_{4,5}$ transitions. Radiative transitions, not shown in this figure, from the $^1D_2$ state to the $^3H_6$,$^3F_2$ levels were also observed. The emission from the $^1D_2$ level shows a strong concentration quenching, and as concentration rises these transitions become very weak if compared with the emissions from the $^3P_0$ level. A similar effect was previously observed in some Pr^{3+}-doped crystals,[17–21] and attributed to cross relaxation between Pr^{3+} ions.

B. Concentration and temperature dependence of lifetimes

In order to obtain additional information about the luminescence properties of Pr^{3+} ions in this crystal, the fluores-

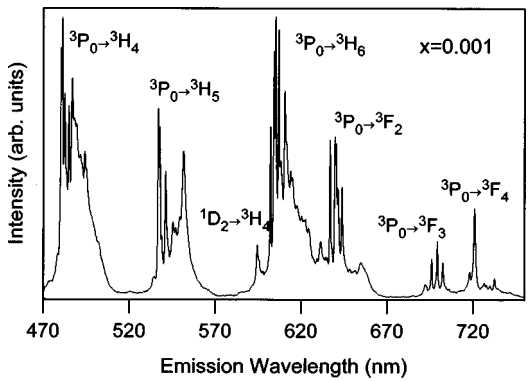

FIG. 2. Time-resolved emission spectrum of the $^3P_0 \rightarrow {}^3H_{4,5,6}$, $^3P_0 \rightarrow {}^3F_{2,3,4}$, and $^1D_2 \rightarrow {}^3H_{4,5}$ transitions of Pr^{3+} in $LiKY_{1-x}Pr_xF_5$ ($x=0.001$) obtained at 1 μs after the laser pulse. Measurements were performed at 4.2 K for an excitation wavelength of 480.5 nm.

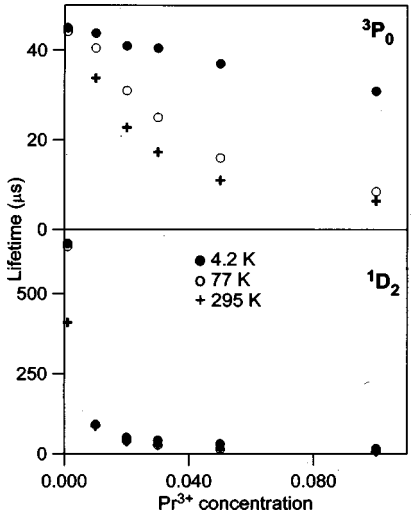

FIG. 3. Lifetime values of $^3P_0$ and $^1D_2$ states as a function of concentration at three different temperatures. Lifetimes were obtained by exciting at 480.5 nm.

cence dynamics of the $^3P_0$ and $^1D_2$ emitting levels was investigated as a function of Pr^{3+} concentration in the 4.2–295 K temperature range. Decay curves for all samples were obtained under laser pulsed excitation at 480.5 nm, and the luminescence was collected in the $^3P_0 \rightarrow {}^3H_6$ and $^1D_2 \rightarrow {}^3H_6, {}^3F_2$ transitions. Figure 3 shows the lifetime values of the $^3P_0$ and $^1D_2$ levels as a function of concentration at three different temperatures (4.2, 77, and 295 K). As can be observed the lifetimes of the $^3P_0$ level are nearly independent on concentration at low temperature; however, those of the $^1D_2$ level, which is about one order of magnitude larger for the less concentrated sample, become shorter with increasing concentration even at low temperature. This variation of fluorescence with concentration indicates the presence of energy transfer processes at concentrations higher than $x=0.001$. The same behavior is observed at 77 and 295 K.

The decays of the $^3P_0$ level can be described at all temperatures and concentrations by an exponential function to a good approximation. Figure 4 shows, as an example, the logarithmic plot of the experimental decays of the $^3P_0$ level (excited at 480.5 nm) at 4.2 K for different Pr^{3+} concentrations.

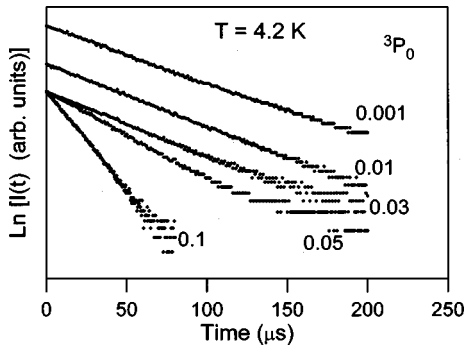

FIG. 4. Logarithmic plot of the fluorescence decays of the $^3P_0$ level for samples doped with $x=0.001$, 0.01, 0.03, 0.05, and 0.1 of Pr^{3+}. The decays were obtained by exciting at the $^3P_0$ level (480.5 nm) at 4.2 K.

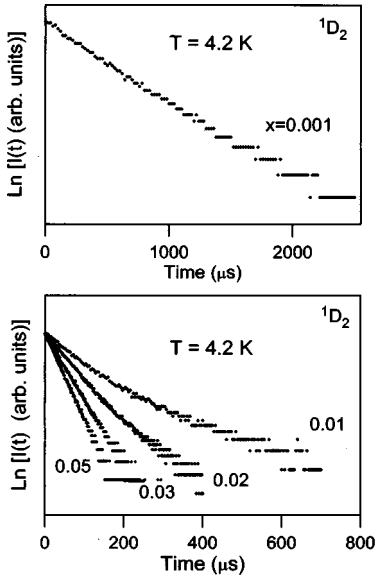

FIG. 5. Logarithmic plot of the fluorescence decays of the $^1D_2$ level for samples doped with $x=0.001$, 0.01, 0.02, 0.03, and 0.05 of Pr^{3+}. The decays were obtained by exciting at the $^3P_0$ level (480.5 nm) at 4.2 K.

The decays of the $^1D_2$ level can be described at a low concentration ($x=0.001$) by an exponential function in the 4.2–295 K temperature range. As concentration increases up to $x=0.02$ the decays become nonexponential and a rapid lifetime decrease occurs; however, for concentrations higher than $x=0.02$ the decays again become single exponential. As an example, Fig. 5 shows the logarithmic plot of the experimental decays of the $^1D_2$ level (excited at 480.5 nm) at 4.2 K for different concentrations.

The lifetime values of the $^3P_0$ level as a function of temperature between 4.2 and 300 K are presented in Fig. 6. As the concentration rises the decays remain exponential but a decrease in the experimental lifetimes is observed between 10 and 77 K. At higher temperatures the lifetimes are nearly constant.

Figure 7 shows the temperature behavior of the $^1D_2$ level for all concentrations. As can be observed in the less concentrated sample ($x=0.001$) the lifetimes vary from 657 to 405 μs between 77 and 295 K. As concentration rises the lifetimes remain nearly temperature independent.

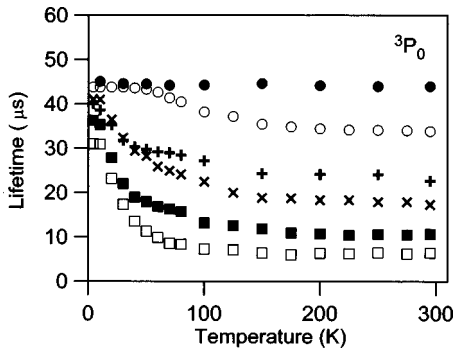

FIG. 6. Temperature dependence of the $^3P_0$ state lifetime of Pr^{3+} ions in $LiKY_{1-x}Pr_xF_5$ crystal: (●) $x=0.001$, (○) $x=0.01$, (+) $x=0.02$, (×) $x=0.03$, (■) $x=0.05$, and (□) $x=0.1$. Lifetimes were obtained by exciting at 480.5 nm.

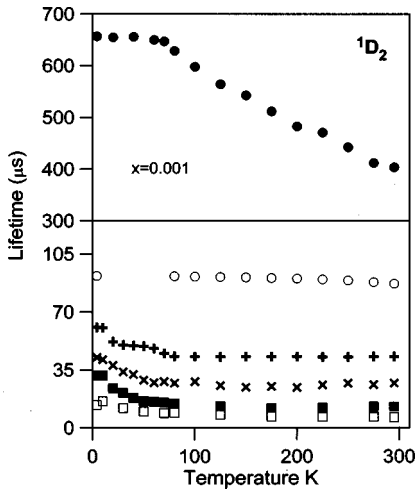

FIG. 7. Temperature dependence of the $^1D_2$ state lifetime of Pr^{3+} ions in $LiKY_{1-x}Pr_xF_5$ crystal: (●) $x=0.001$, (○) $x=0.01$, (+) $x=0.02$, (×) $x=0.03$, (■) $x=0.05$, and (□) $x=0.1$. Lifetimes were obtained by exciting at 480.5 nm.

C. Quenching of the $^3P_0$ emission

Concentration quenching of fluorescence from the $^3P_0$ level of Pr^{3+} in $LiKYF_5$ crystal has been studied starting from lifetime results. This nonradiative process is also temperature dependent between 10 and 77 K.

The $^3P_0$ emission can be quenched by three different processes: (i) Relaxation by multiphonon emission to the $^1D_2$ level, (ii) cross relaxation between pairs of Pr^{3+}, populating either the $^1D_2$ level or the $^1G_4$ level, and (iii) energy migration to quenching sites. The latter two depend on the concentration of Pr^{3+} ions in the lattice.

As we have seen in the emission spectrum (Fig. 2), at low concentration the emission spectrum contains a small amount of $^1D_2$ emission in addition to the $^3P_0$ emission. Population of the $^1D_2$ level after $^3P_0$ excitation can take place via processes (i) and (ii). The first nonradiative channel to be considered is multiphonon relaxation. The energy difference between $^3P_0$ and $^1D_2$ levels is around 3500 cm^{-1} and the highest frequency of the lattice phonons is 440 cm^{-1}, hence at least eight phonons are needed in the process. The rate of multiphonon relaxation can be estimated from the modified energy gap law[22]

$$W_{\mathrm{MPR}}=\beta_{el}\exp[-\alpha(\Delta E-2\hbar\omega_{\max})], \tag{1}$$

where α and β_{el} are constants, ΔE is the energy gap to the next lower manifold, and $\hbar\omega_{\max}$ is the maximum energy of the optical phonons. Using the values[22] of $\alpha=4.5\times10^{-3}$ and $\beta_{el}=10^7$, a value of $2\times10^2\ s^{-1}$ is obtained, which indicates that this process can not compete with the radiative relaxation of the $^3P_0$ level ($\approx2\times10^4\ s^{-1}$).

The second nonradiative channel to be considered is cross-relaxation of the $^3P_0$ level via $[^3P_0,{}^3H_4]\rightarrow[^1D_2,{}^3H_6]$ or $[^3P_0,{}^3H_4]\rightarrow[^1G_4,{}^1G_4]$ processes. From absorption and luminescence spectra we found the energy mismatch of the $[^3P_0,{}^3H_4]\rightarrow[^1D_2,{}^3H_6]$ process to be about -820 cm^{-1} making this quenching mechanism ineffective at 4.2 K. On the other hand, the $[^3P_0,{}^3H_4]\rightarrow[^1G_4,{}^1G_4]$ process can also be disregarded because spectroscopic data reveal an energy mismatch of about 900 cm^{-1}.

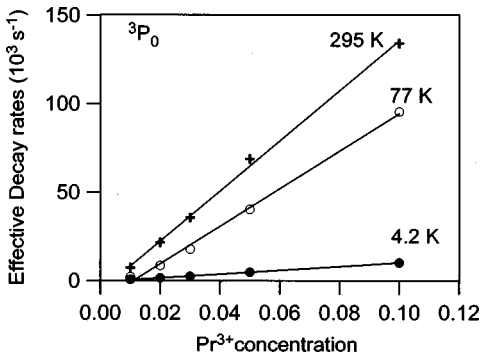

FIG. 8. Effective decay rates of the $^3P_0$ emission as a function of Pr^{3+} concentration at three different temperatures.

An examination of the energy level diagram in Fig. 1 and the emission spectrum in Fig. 2 suggests that a possible explanation for the concentration quenching of emission $^3P_0$ could be a cross relaxation via the $[^3P_0,{}^3H_4]\rightarrow[^3H_6,{}^1D_2]$ process, because the energy mismatch is less than 100 cm^{-1}. This process begins with one Pr^{3+} ion (the donor) in the $^3P_0$ excited state and another one (the acceptor) in the ground state $^3H_4$. In a simultaneous nonradiative process, the donor makes a transition to $^3H_6$ whereas the acceptor is excited to $^1D_2$. An inspection of the energy of the Stark levels of the $^3H_4$, $^3H_6$, and $^1D_2$ manifolds derived from the absorption and emission measurements (Figs. 1 and 2) shows that the $^3P_0(20816\ cm^{-1})\rightarrow{}^3H_6(1)(4269\ cm^{-1})$ transition is nearly resonant with the

$$^3H_4(2)(30\ cm^{-1})\rightarrow{}^1D_2(1)(16\,609\ cm^{-1})$$

transition [(1) represents the lowest Stark levels of the $^3H_6$ and $^1D_2$ states and (2) the second Stark level of $^3H_4$ state], with a thermal activation energy of 30 cm^{-1} and a mismatch of -32 cm^{-1}. On the other hand, as mentioned in Sec. III B, for samples with Pr^{3+} concentrations higher than $x=0.01$ the decays of the $^3P_0$ state increase between 10 and 77 K suggesting the onset of a thermal activation process.[23] The decay rate W for such activation process can be described by the relation

$$W=Ae^{-\Delta/KT}, \tag{2}$$

where Δ is the activation energy and A is a constant. A plot of the measured decay rates as a function of $1/T$ in the 10–77 K temperature range gives an activation energy of about 30 cm^{-1}, which has the same value as the one for the $[^3P_0,{}^3H_4(2)]\rightarrow[^3H_6(1),{}^1D_2(1)]$ process. Therefore, we conclude that this could be the most probable process explaining the thermal quenching of the $^3P_0$ emission.

Finally let us consider energy migration. As we mentioned in Sec. III B, the decay times of the $^3P_0$ level were single exponential for all concentrations and temperatures. In the diffusion model,[24,25] in the case of the dipole-dipole interaction with very fast diffusion, the decay of the donor fluorescence is purely exponential and the effective decay shows a linear dependence on concentration. In our case the donors and acceptors are the Pr^{3+} ions.

Figure 8 shows the effective fluorescence decay times as a function of the Pr^{3+} concentration. As can be observed, in this concentration range, the effective decay rates show a

linear dependence on concentration in the 4.2–295 K temperature range, which indicates that the behaviour is close to a dipole-dipole quenching mechanism in the framework of a fast-diffusion regime.

D. Concentration quenching of the $^1D_2$ emission

The emission from the $^1D_2$ level shows a strong concentration quenching, and as concentration rises the emission becomes very weak if compared with the emissions from the $^3P_0$ level. A similar effect was previously oberved in some Pr^{3+}-doped crystals,[17–21] and attributed to cross relaxation between Pr^{3+} ions. The $[^1D_2,^3H_4]\rightarrow[^1G_4,^3F_{3,4}]$ cross relaxation channel is more efficient than the $[^3P_0,^3H_4]\rightarrow[^1G_4,^1G_4]$ channel because the energy mismatch between the levels involved in the latter process is much larger than for the former.

As we mentioned in Sec. III B, lifetime measurements show that at low temperatures and low concentrations ($x=0.001$) the $^1D_2$ emission lifetime is single exponential, and should approach the radiative lifetime of the $^1D_2$ level because the multiphonon relaxation rate for this level is expected to be small due to the high-energy gap to the next lower lying J manifold (6500 cm^{-1}) and the values of phonon energies involved (440 cm^{-1}). As the concentration rises, the lifetime decreases even at 4.2 K (see Fig. 3), which indicates that Pr-Pr relaxation processes are present at concentrations higher than $x=0.001$. The decays become nonexponential as concentration increases up to $x=0.02$; however, beyond $x=0.02$ the decays are again single exponential showing that diffusion processes could be competitive with a direct transfer at high concentrations.

In order to identify the energy transfer mechanism between Pr^{3+} ions we have analyzed the experimental decays of the $^1D_2$ level for the samples doped with $x=0.01$ and $x=0.02$ where a limited diffusion process may occur. Under the assumption of electrostatic multipole interaction the donor decay curves can be described by the expression[26]

$$I(t)=I(0)\exp\left[-\frac{t}{\tau_0}-\Gamma\left(1-\frac{3}{s}\right)\frac{4}{3}\pi R_0^3 N\left(\frac{t}{\tau_0}\right)^{3/s}-Wt\right], \tag{3}$$

with $s=6$, 8, and 10, respectively, for electric dipole-dipole, dipole-quadrupole, and quadrupole-quadrupole interactions. τ_0^{-1} is the intrinsic decay rate, $\Gamma(x)$ is the gamma function evaluated in x, N is the donor concentration, R_0 is the critical transfer distance defined as the distance for which the probability for energy transfer between a given donor-acceptor pair is equal to the donor intrinsic decay probability, and W is the probability of migration-limited relaxation. The intrinsic decay time τ_0^{-1} is obtained from the low-temperature decay of the less concentrated sample ($x=0.001$) which is single exponential. The decay curves for the samples doped with $x=0.01$ and 0.02 were fitted to Eq. (3) with the critical radius R_0 and the rate of migration limited energy transfer W as variable parameters for $s=6$, 8, and 10.

Figure 9 shows a least square fit of the experimental decay at 4.2 K to Eq. (3) for two different Pr^{3+} concentrations ($x=0.01$ and 0.02). In both samples the best fit obtained was for $s=6$ at all temperatures (4.2–295 K). The obtained values for R_0 were 1.04 and 0.595 nm, respectively. The migration transfer rates were found to be $W=7\times10^3\,s^{-1}$ ($x=0.01$) and $W=15\times10^3\,s^{-1}$ ($x=0.02$), respectively. For the sample doped with $x=0.01$ the energy migration rate takes the same value at 77 and 295 K, whereas for $x=0.02$ increases from $15\times10^3\,s^{-1}$ at 4.2 K to $21\times10^3\,s^{-1}$ at 77 and 295 K. The temperature dependence of the rate of energy migration has been examined by Weber in Ref. 24. This rate depends on the frequencies, linewidths, and probabilities of all the transitions between the levels $^1D_2$ and $^3H_4$. Account taken of the complexity of the $^1D_2\rightarrow{}^3H_4$ transition it is difficult to evaluate the expected temperature dependence of these quantities and therefore to explain the observed behavior of the energy migration rate.

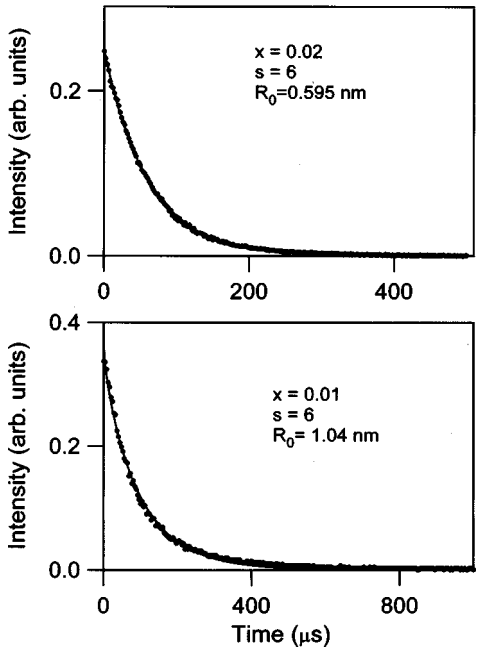

FIG. 9. Experimental emission decay curves of $^1D_2$ level and the calculated fit for dipole-dipole interaction ($s=6$) (solid line) for the samples doped with $x=0.01$ and 0.02 of Pr^{3+} at 4.2 K.

For the sample doped with $x=0.02$, reasonable fits to the dipole-quadrupole and quadrupole-quadrupole interactions can be obtained. These fits are poorer than the one obtained with a dipole-dipole interaction but are close enough and give the same values for R_0 and W, so it is difficult to say unambiguously that only dipole-dipole interactions are responsible for the transfer at this concentration. However, as can be observed, a dipole-dipole transfer mechanism is consistent with the experimental decays for these concentrations.

As we mentioned before for concentrations higher than $x=0.02$, the experimental decays become again single exponentials. This behavior could be associated with a rapid energy diffusion between Pr^{3+} ions. In the transfer rapid limit the donor transfer takes place so quickly that transfer times for different donor-acceptor pairs are averaged out and the whole system exhibits a single exponential decay as is experimentally observed.[24] This is also supported by the linear dependence of the effective decay rate of the $^1D_2$ state as a function of Pr^{3+} concentration ($x>0.02$) as is shown in Fig. 10.

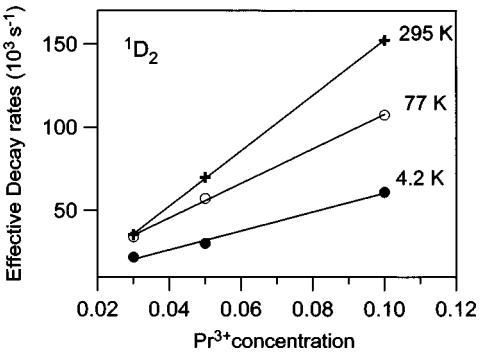

FIG. 10. Effective decay rates of the $^1D_2$ emission as a function of Pr^{3+} concentration ($x>0.02$) at three different temperatures.

E. Upconversion

To investigate the possibility of up-converted fluorescence in this crystal we have directly excited the $^1D_2$ level and we have observed anti-Stokes fluorescence from the $^3P_0 \rightarrow {}^3H_4$ transition in the 4.2–295 K temperature range for different Pr^{3+} concentrations. Figure 11 shows the up-converted emission for the sample doped with $x=0.02$ at 4.2 K. The spectrum shows three main peaks. The Stark components theoretically expected for the C_2 symmetry site are not completely resolved, probably due to the spectral resolution of the measurements. The intensity of the anti-Stokes emission shows a close quadratic dependence with the excitation laser energy which indicates that two photons participate in the upconversion process. Figure 12 shows the integrated emission intensity of the up-converted fluorescence as a function of the square of the laser energy.

The upconversion process can occur via two distinct mechanisms: radiatively by an excited-state absorption (ESA) or nonradiatively by an energy transfer upconversion (ETU).[27,28] In the first mechanism a single ion is involved whereas two ions are involved in the second one. As two laser photons are involved in each of the above processes, the $^3P_0$ fluorescence shows a quadratic dependence on pump laser energy as has been observed in various systems.[29–34] Lifetime measurements provide an invaluable tool in discerning which is the operative mechanism. The radiative ESA process occurs within the excitation pulse width, leading to an immediate decay of the upconversion luminescence

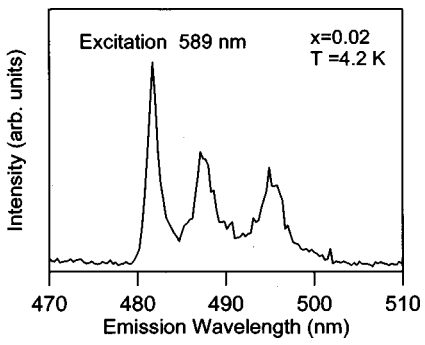

FIG. 11. Fluorescence spectrum corresponding to the $^3P_0 \rightarrow {}^3H_4$ transition at 4.2 K. The excitation wavelength (589 nm) was in resonance with the transition $^3H_4 \rightarrow {}^1D_2$. (Sample with $x=0.02$).

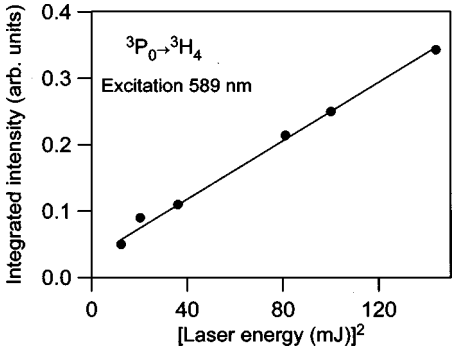

FIG. 12. Fluorescence intensity of the up-converted $^3P_0 \rightarrow {}^3H_4$ emission as a function of the square of the excitation energy. Data correspond to 4.2 K and $x=0.02$ of Pr^{3+}.

after excitation. Up-conversion by energy transfer leads to a decay curve for the anti-Stokes emission which shows a rise time after the laser pulse, followed by a decay and a lifetime longer than that of the $^3P_0$ level under direct excitation. These effects become more pronounced as the $^1D_2$ lifetime increases.[30] This distinction is possible when the pulse width is much shorter than the time constant of the relevant energy transfer step.[35]

The time evolution of the upconverted emission from the $^3P_0$ level obtained after excitation in the $^1D_2$ state shows the latter behavior. Figure 13 shows the decays of $^3P_0$ emission after excitation into the $^1D_2$ level for three different concentrations at 295 K. The decay curves of the anti-Stokes $^3P_0 \rightarrow {}^3H_4$ emission show a certain delay (or rise) time which decreases as Pr^{3+} concentration increases. As the concentration increases the interionic distance decreases and hence the energy transfer probability increases. Therefore, the rise time decreases with concentration since the transfer rate is the inverse of time. It must also be noted that the delay time depends on the lifetimes of the levels involved in the energy transfer process. The observed rise time of the $^3P_0$ decays obtained under pulsed excitation in the $^1D_2$ state indicates that the energy transfer process is responsible for the anti-Stokes fluorescence of Pr^{3+} in $LiKYF_5$ crystal.

Two different mechanisms have been proposed to account for this ETU process.[36,37] One of them involves levels $^3H_4$, $^3H_6$, $^1D_2$, and $^3P_0$. In this process an ion in the $^3H_6$ state (populated upon relaxation from the $^1D_2$ state) annihilates with a nearby ion in the $^1D_2$ state resulting in one ion in the $^3H_4$ ground state and the other one in the excited $^3P_0$ state where upconverted fluorescence occurs. In this model the rate equations describing the time dependence of the populations of each level are the following:

$$\frac{dN_2}{dt} = -\frac{N_2}{\tau_2} - \sigma_u N_2 N_1,$$

$$\frac{dN_1}{dt} = \sigma_{21} N_2 - \frac{N_1}{\tau_1} - \sigma_u N_2 N_1, \tag{4}$$

$$\frac{dN_3}{dt} = \sigma_u N_2 N_1 - \frac{N_3}{\tau_3},$$

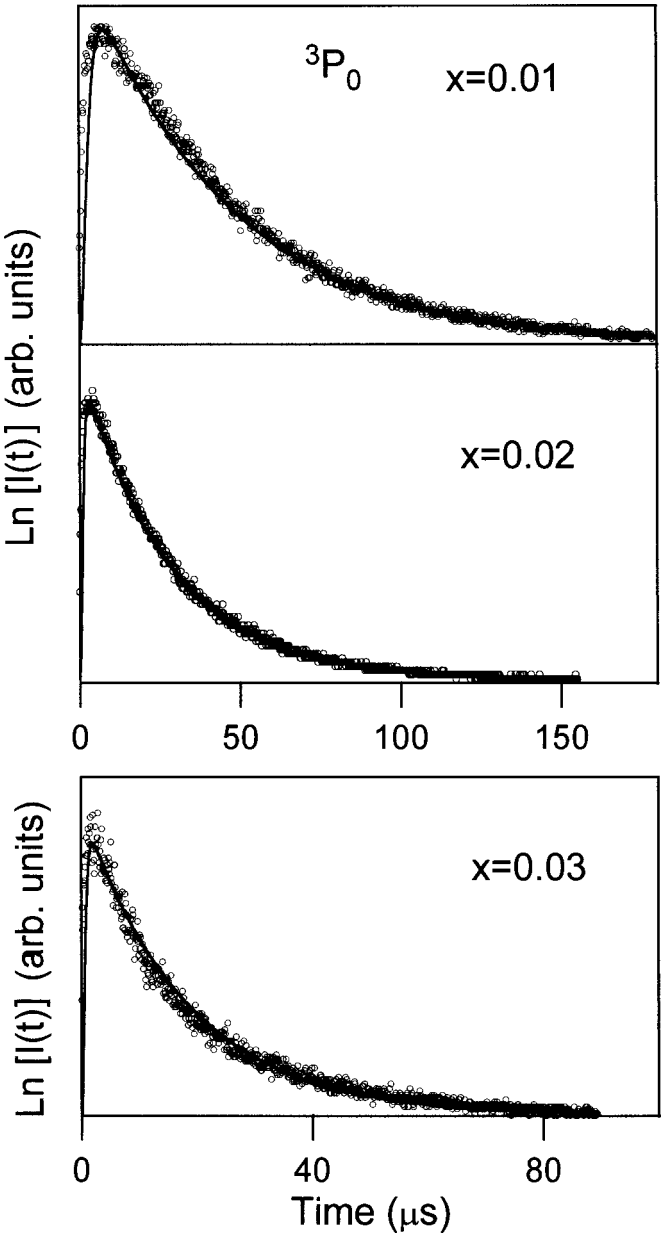

FIG. 13. Fluorescence decays of the up-converted $^3P_0 \rightarrow {}^3H_4$ emission after excitation of the $^3H_4 \rightarrow {}^1D_2$ absorption for three different concentrations $x=0.01$, 0.02, and 0.03. Data correspond to room temperature. Symbols stand for the experimental data and solid lines correspond to the numerical solutions of $N_3(t)$ obtained from Eqs. (4).

where τ_1, τ_2, and τ_3 are the lifetimes of $^3H_6$, $^1D_2$, and $^3P_0$ levels, σ_{21} the transition probability rate constant from $^1D_2$ to $^3H_6$, and σ_u the rate constant for the ETU process.

The $^1D_2$ state is resonantly excited at $t=0$, so initially population exists only in this level. In a first step to reduce the complexity of solutions we have assumed that the population of $^1D_2$ and $^3H_6$ levels by decay from $^3P_0$ is insignificant and that the up-conversion rate constant is small when compared to intrinsic decay rate. Under these conditions, the solution of the rate equation for the population of level $^3P_0$ is given by

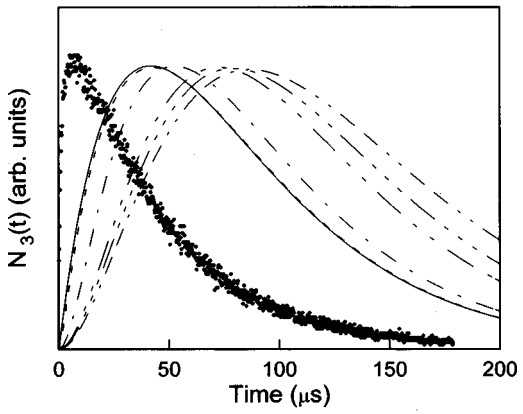

FIG. 14. Fluorescence decays of the up-converted $^3P_0 \rightarrow {}^3H_4$ emission after excitation of the $^3H_4 \rightarrow {}^1D_2$ absorption for $x=0.01$. Data correspond to room temperature. Symbols stand for the experimental data and lines correspond to a fit with Eq. (4) with different values for τ_1: (—) 0.1 μs, (---) 1 μs, (— — —) 10 μs, (— - — - —) 40 μs, (— — — —) 60 μs, and (— — —-) 100 μs.

$$N_3(t)=\frac{\sigma_u\sigma_{21}N_2^2(0)}{(\tau_1^{-1}-\tau_2^{-1})}\left[\frac{\exp(-2t/\tau_2)}{(\tau_3^{-1}-2\tau_2^{-1})}-\frac{\exp[-t(\tau_1^{-1}+\tau_2^{-1})]}{(\tau_3^{-1}-\tau_2^{-1}-\tau_1^{-1})}+\frac{(\tau_1^{-1}-\tau_2^{-1})}{(\tau_3^{-1}-2\tau_2^{-1})}\frac{\exp(-t/\tau_3)}{(\tau_3^{-1}-\tau_2^{-1}-\tau_1^{-1})}\right]. \quad (5)$$

The time dependence of $N_3(t)$ for the upconversion process according to Eq. (5) is shown in Fig. 14, which also includes the experimental decay for the sample doped with $x=0.01$ of Pr^{3+}. This calculation was made by using different values for τ_1 (the unknown lifetime of the $^3H_6$ state) and the experimental values for the $^1D_2$ and $^3P_0$ levels. As can be observed the decay and rise time predicted by this model, assuming the upconversion rate constant to be small compared to the intrinsic decay rates, is too large to account for the observed experimental behavior of the decays.

If we take into account the possibility of a regime where the up-conversion rate constant is significant compared to the intrinsic decay rates, no analytical solution can be found. In this case, a numerical solution can be obtained for the transient behavior of the population of the $^3P_0$ level taking τ_1, σ_{21}, and σ_u as parameters, and using the experimental lifetimes of $^1D_2$ and $^3P_0$ levels. As the lifetime value of the $^3H_6$ level does not have a great influence on the solution, a value of $\tau_1=100\,\mu$s was taken for computational purposes. Figure 13 compares the numerical solution of $N_3(t)$ to the experimental values for three different Pr^{3+} concentrations. Table I summarizes the fitted values for σ_u and σ_{21} parameters together with the experimental lifetimes of $^1D_2$ and

TABLE I. Summary of the fitted values for σ_u and σ_{21} parameters together with the experimental lifetimes of $^1D_2(\tau_2)$ and $^3P_0(\tau_3)$ levels.

x	τ_2 (μs)	τ_3 (μs)	σ_u (s)$^{-1}$	σ_{21} (s)$^{-1}$
0.01	87	40	8.6×10^5	2.5×10^7
0.02	43	23	6.5×10^6	4.3×10^7
0.03	27	18	2.0×10^7	8.0×10^7

$^3P_0$ levels. As can be observed, a good fit of the experimental decays is obtained. However, the fitted values for the transition probability rate $^1D_2 \rightarrow {}^3H_6(\sigma_{21})$, shown in Table I, are three orders of magnitude larger than the experimental decay rates of the $^1D_2$ level. This inconsistency could be related to the existence of some other processes feeding the $^3P_0$ level which are not considered in this model.

The second process[37] proposed to explain the ETU, considers the transfer inside pairs of ions after selective excitation by a pulsed laser. In this model, when both ions of a pair are excited to the $^1D_2$ state, a transfer occurs by which one ion loses energy and goes to the lower excited level $^1G_4$, while the other one gains energy and goes to the $^3P_2$ level from where, by nonradiative decay the $^3P_0$ level is populated. Although this model also gives a good fit to the experimental decays for the up-converted fluorescence, the existence of a fast-diffusion regime found in most of the samples (see Sec. III) makes it inadequate to explain the ETU process.

IV. CONCLUSIONS

From the above results, the following conclusions can be reached.

(i) Although it is difficult to single out the dominant mechanism responsible for the fluorescence quenching of the $^3P_0$ level due to the large number of levels involved, the temperature-dependent concentration quenching of the $^3P_0$ fluorescence in the 10–77 K temperature range for Pr^{3+} concentrations higher than $x=0.01$ can be described in the framework of a thermally activated cross-relaxation process involving the $^1D_2$ and $^3H_6$ states. However, the single exponential character of the decays together with the linear dependence on concentration of the effective decay rates suggest that energy migration is also present in this system.

(ii) Fluorescence quenching from the $^1D_2$ state has been demonstrated to occur for Pr^{3+} concentrations higher than $x=0.001$ even at 4.2 K. This can be attributed to a cross relaxation process. The time evolution of the decays from the $^1D_2$ state is consistent with a dipole-dipole energy transfer mechanism.

(iii) Anti-Stokes fluorescence from the $^3P_0 \rightarrow {}^3H_4$ transition under excitation of the $^1D_2$ level was observed. The rise time observed in the $^3P_0$ decays shows that this level is populated from lower lying levels and supports the argument that energy transfer is responsible for the up-conversion process. However, this process seems to be complex enough to allow for the use of a single model which could explain the behavior observed.

ACKNOWLEDGMENTS

We would like to thank E. Montoya (Departamento de Física de Materiales of the Autonomous University of Madrid) for his assistance with upconversion measurements. This work was supported by the Spanish Government (DGICYT Ref. No. PB95-0512), and CICYT (Ref. No. MAT97-1009).

[1] A. A. Kaminskii, Ann. Phys. (Paris) **16**, 639 (1991).
[2] A. Bleckmann, F. Heine, J.-P. Meyn, T. Danger, E. Heumann, and G. Huber, in *OSA Proceedings on Advanced Solid-State Lasers*, edited by A. A. Pinto and T. Y. Fan (OSA, Washington, D.C., 1993), Vol. 15, pp. 199–201.
[3] M. Malinowski, M. F. Joubert, and B. Jacquier, Phys. Status Solidi A **140**, K49 (1993).
[4] M. E. Koch, A. W. Kueny, and W. E. Case, Appl. Phys. Lett. **56**, 1083 (1990).
[5] R. G. Smart, D. C. Hanna, A. C. Tropper, S. T. Davey, S. F. Carter, and D. Szebesta, Electron. Lett. **127**, 1307 (1991).
[6] M. Malinowski, M. F. Joubert, and B. Jacquier, Phys. Rev. B **50**, 12 367 (1994).
[7] J. Y. Allain, M. Monerie, and H. Poignant, Electron. Lett. **27**, 189 (1991).
[8] L. Esterowicz, R. Allen, M. Kruer, F. Bartoli, L. S. Goldberg, H. P. Jenssen, A. Linz, and V. O. Nicolai, J. Appl. Phys. **48**, 650 (1997).
[9] J. Hegarty and W. M. Yen, J. Appl. Phys. **51**, 3545 (1980).
[10] A. A. Kaminskii, B. P. Sobolev, T. V. Uvarova, and M. I. Chertanov, Neorg. Mater. **20**, 703 (1984).
[11] A. A. Kaminskii, A. A. Markosyan, A. V. Pelevin, Yu A. Poliakova, S. E. Sarkisov, and T. V. Uvarova, Neorg. Mater. **22**, 870 (1986).
[12] A. A. Kaminskii, V. S. Mironov, S. N. Bagaev, N. M. Khaidukov, M. F. Joubert, B. Jacquier, and G. Boulon, Phys. Status Solidi A **145**, 177 (1994).
[13] J. F. H. Nicholls, X. X. Zhang, M. Bass, B. H. T. Chai, and B. Henderson, Opt. Commun. **137**, 281 (1997).
[14] A. V. Gorunov, A. I. Popov, and N. M. Khaidukov, Mater. Res. Bull. **27**, 213 (1992).
[15] P. P. Fedorov, M. D. Valkovskii, L. B. Medvedeva, O. S. Bondareva, N. M. Khaidukov, and B. P. Sobolev, Neorg. Mater. **38**, 432 (1993).
[16] H. Weidner, J. F. H. Nicholls, W. A. McClintic, Jr., M. McKaig, K. M. Beck, B. H. T. Chai, N. M. Khaidukov, and R. E. Peale, in *Advanced Solid State Lasers*, edited by B. H. T. Chai and S. A. Payne (Optical Society of America, Washington, D.C., 1995), pp. 545–550.
[17] H. Dornauf and J. Heber, J. Lumin. **22**, 1 (1980).
[18] C. de Mello Donega, H. Lambaerts, A. Meijerink, and G. Blasse, J. Phys. Chem. Solids **54**, 873 (1993).
[19] C. de Mello Donega, A. Ellens, A. Meijerink, and G. Blasse, J. Phys. Chem. Solids **54**, 293 (1993).
[20] A. Lorenzo, L. E. Bausá, and J. García Solé, Phys. Rev. B **51**, 16 643 (1995).
[21] B. Savoini, J. E. Muñoz Santiuste, and R. González, Phys. Rev. B **56**, 5856 (1997).
[22] J. M. F. van Dijk and M. F. H. Schuurmans, J. Chem. Phys. **78**, 5317 (1983).
[23] J. Hegarty, D. L. Huber, and W. M. Yen, Phys. Rev. B **25**, 5638 (1982).
[24] M. J. Weber, Phys. Rev. B **4**, 2932 (1971).
[25] F. Auzel, in *Radiationless Processes*, edited by B. Di Bartolo (Plenum, London, 1980), p. 213.
[26] D. L. Dexter, J. Chem. Phys. **21**, 836 (1953).
[27] F. Auzel, Proc. IEEE **61**, 758 (1973).
[28] J. C. Wright, Top. Appl. Phys. **15**, 239 (1976).

[29] J. Ganem, W. M. Dennis, and W. M. Yen, J. Lumin. **54**, 79 (1992).
[30] O. L. Malta, E. Antic-Fidancev, M. Lemaitre-Blaise, J. Dexpert-Ghys, and B. Piriou, Chem. Phys. Lett. **129**, 557 (1986).
[31] E. M. Pacheco and C. B. Araujo, Chem. Phys. Lett. **148**, 334 (1988).
[32] L. E. E. de Araujo, A. S. L. Gomes, Cid B. de Araujo, Y. Messaddeq, A. Florez, and M. A. Aegerter, Phys. Rev. B **50**, 16 219 (1994).
[33] M. Malinowski, C. Garapon, M. F. Joubert, and B. Jacquier, J. Phys.: Condens. Matter **7**, 199 (1995).
[34] J. A. Capobianco, N. Raspa, A. Monteil, and M. Malinowski, J. Phys.: Condens. Matter **5**, 6083 (1993).
[35] M. Wermuth, T. Riedener, and H. U. Gudel, Phys. Rev. B **57**, 4369 (1998).
[36] D. J. Zalucha, J. C. Wright, and F. K. Fong, J. Chem. Phys. **59**, 997 (1973).
[37] B. Buisson and J. C. Vial, J. Phys. (France) Lett. **42**, L115 (1981).